Probabilistic Damage Detection Based on Large Area Electronics Sensing Sheets

Yao Yao, Branko Glisic

7th European Workshop on Structural Health Monitoring
July 8-11, 2014. La Cité, Nantes, France

Probabilistic Damage Detection Based on Large Area Electronics Sensing Sheets

Yao Yao and Branko Glisic

Department of Civil and Environmental Engineering at Princeton University

Abstract

Reliable early-stage damage detection and characterization requires continuous sensing over large areas of structure. The limitations with current sensing technologies lies in the fact that they either have high cost and insufficient spatial resolution, or rely on complex algorithms that are challenged by varying environmental and loading conditions. This paper addresses the need for direct sensing where anomalies are sensed at close proximity through a dense array of sensors, and proposes one approach for sensor network design. This approach is directly applicable to innovative sensing sheet based on large area electronics (LAE), which enables practical implementation of dense arrays of sensors. However, although the sensors are densely spaced in the sensing sheet, there are still some non-instrumented spaces between them and these spaces are not sensitive to damage. In this research, a probabilistic approach based on Monte Carlo (MC) simulations is researched to determine the probability that damage of certain size that occurs within the area covered by the sensing sheet can be detected with a given sensor network. Based on these Probability of Detection (POD) functions, it was possible to assess the reliability of sensing sheets for crack detection and to establish general principles for the design of sensing sheets.

Keywords: structural health monitoring; probabilistic damage detection; direct sensing; large area electronics; Monte Carlo method

1. Introduction

1.1 Direct sensing approach

Civil infrastructure provides essential welfare in society and its structural safety and performance are of highest importance. Structural health monitoring (SHM) is a potentially an effective method for assessment of structures, if it can supply low-cost sensing technologies that provide reliable and actionable information on structural performance and condition. SHM methods can facilitate early identification of potential structural problems and improve the optimization and preparation of appropriate maintenance procedures.

In general, there are two main approaches for damage detection: (1) indirect sensing, and (2) direct sensing [1]. The indirect sensing approach is based on measurements made by sensing media that are not in direct contact with damage. The recorded data is analyzed using various classes of algorithms in order to ascertain damage detection and perform damage characterization. The advantage of this approach is the need for a relatively small number of sensors. However, the main challenge with indirect sensing is the need for sophisticated data-processing algorithms to achieve the spatial resolutions and detection localizations that are required in practical SHM applications [2]. The direct sensing approach is based on measurements made by sensing media that are in direct contact with damage, and thus the damage is detected and localized directly as an unusual change in the output from the sensors affected by the crack. The advantage of this approach is its very high reliability in damage detection and characterization [3-4]; however, the challenge is that this approach requires a large amount of densely placed sensors, which can increase the overall cost and complexity of SHM.

Both direct and indirect sensing have advantages and challenges; however, with the

development of new sensing technologies, low-cost direct sensing has the potential to become reality and to play an important role in damage detection and characterization. The research hypothesis is that by substantially increasing the sensor response to local anomalies, direct sensing leads to greater robustness than current state-of-the-art approaches.

This research focuses to crack detection based on dense arrays of strain sensors. At present, three categories of strain sensors are commercially available [1]: discrete short-gauge sensors, discrete long-gauge sensors, and continuous (1D) distributed sensors (or sensing cables). In addition, there is other ongoing research in the development of continuous 2D sensors (sensing sheets, sensing skins, paints, self- sensitive materials, etc.). A schematic comparison between the damage detection capabilities of various types of sensors is given in Figure 1.

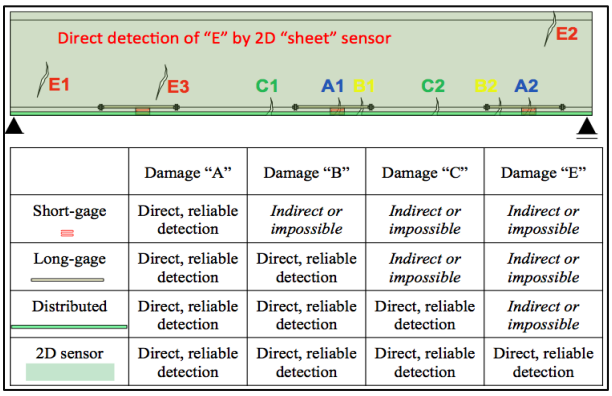

	Damage "A"	Damage "B"	Damage "C"	Damage "E"
Short-gage	Direct, reliable detection	*Indirect or impossible*	*Indirect or impossible*	*Indirect or impossible*
Long-gage	Direct, reliable detection	Direct, reliable detection	*Indirect or impossible*	*Indirect or impossible*
Distributed	Direct, reliable detection	Direct, reliable detection	Direct, reliable detection	*Indirect or impossible*
2D sensor	Direct, reliable detection	Direct, reliable detection	Direct, reliable detection	Direct, reliable detection

Figure 1. Schematic comparison between damage detection capabilities of short-gauge, long-gauge, and 1D distributed sensors, and the need for 2D sensing sheets [1].

1.2 Sensing sheets based on LAE

Large area electronics (LAE) is an emerging technology that allows a broad range of electronic devices to be integrated on low-cost plastic sheets [5-6]. Through the use of micro-fabrication techniques, thin-film sensors have been demonstrated (including strain sensors, pressure sensors, vapor sensors, particle sensors, etc.). These sensors can be formed into dense arrays spanning large areas (i.e., tens of square meters). LAE can potentially be an invaluable tool for damage detection and characterization in large-scale structures [7]. Current commercially available direct sensing techniques that are based on strain measurements either monitor cracks at one point or segment (e.g. short-gauge and long-gauge sensors), or in one dimension (1D, e.g., distributed Fiber Optic sensors). LAE sensing sheets can be treated as a quasi-distributed sensor in two dimensions (2D). The concept of a sensing sheet and its application are schematically shown in Figure 2.

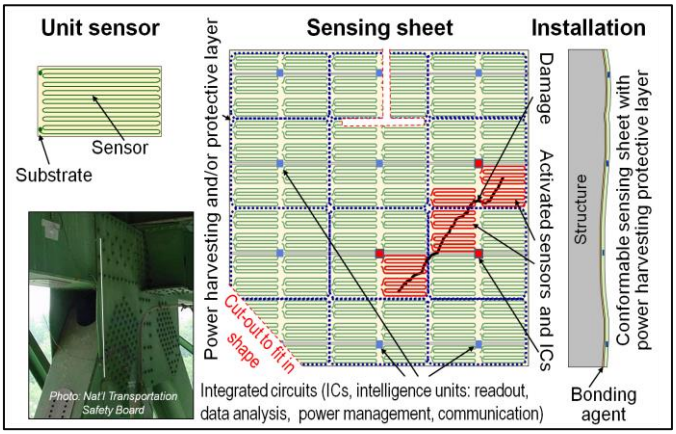

Figure 2. Schematic representation of the sensing sheet based on LAE and ICs.

Sensing sheets consist of the following: (1) a two-dimensional dense array of unit strain

sensors patterned on a polyimide substrate and combined with functional LAE; (2) embedded integrated circuits (ICs) interfaced via non-contact links for sensor readout, data analysis, power management, and communication; and (3) an integrated flexible photovoltaic sheet and power converters (rechargeable batteries) on the LAE sheet to power the full system and protect it from elements.

1.3 Problem statement

Sensing sheets consist of dense array of 2D-distributed individual discrete sensors, but although the sensors are densely spaced, there are some empty spaces between them and these spaces are not sensitive to minute damage. Probabilistic approaches in damage detection can help practical evaluation of the damage. The probability of detection (POD) is essentially a metric used to quantify the reliability of inspection systems, so the effectiveness of different SHM techniques is usually characterized by a POD curve that relates the size of damage to the probability of correct detection [8]. The specific objective of this paper will be achieved through research and creation of POD curves for determination of an optimal design of sensing sheets in terms of number and area of sensors. The probability of crack detection for a single sensor in the sensing sheet was determined first from an analytical (geometrical) solution, and then two numerical solutions based on Monte Carlo simulation (MCS) were created. The analytical and numerical solutions were mutually validated for the single sensor case. Then the validated MCS was extended to study the cases with multiple sensors in the sensing sheet. We believe that the presented research provides important references for an optimal sensing sheet design. In addition, far beyond the specific objective of the project, it contributes significantly to the field of POD and creates a foundation for the study of multiple-sensor arrangements, which can be applied in various strain-based SHM applications.

2. Methodology and its validation

In order to build analytical and numerical models for determination of the POD for a crack with length *L* (denoted with *POD(L)*)), occurring in the sensing sheet with dimensions *BxH*, which is instrumented with individual sensors, each with dimensions *bxh*, the following idealized assumptions were adopted:

- The location of the crack center is uniformly distributed over the entire area;
- The crack orientation is uniformly distributed between 0 and π;
- The crack length is uniformly distributed;
- The crack is idealized as a straight line;
- Detection happens if the crack "touches" any part of the sensor;
- No false positives are possible (e.g. the sensor cannot detect a crack that is not there).

The above assumptions are schematically presented in Figure 3 for single sensor case. All three cracks in the figure have the same probability of occurrence. The two cracks to the left/lower left of the sensor will be detected, while the crack in the upper right corner will not be detected.

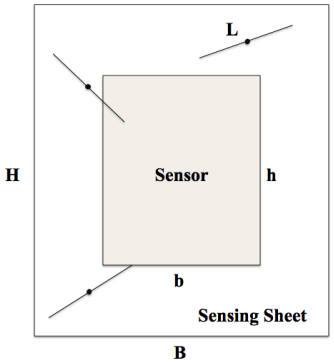

Figure 3. Idealized model of the probabilistic crack detection, single sensor case.

The creation of analytical and numerical models was approached geometrically. For a given crack length L, if a crack position and orientation is within detectable angle, the sensor will detect the crack. If the crack center (the black dot in left image of Figure 4) is within the sensor area it will be reliably detected since all angles are detectable angles. On the other hand, if the crack center is too far from the sensor, it will have no detectable angles and its probability of detection is zero. These "detectable angles" are shown as the shaded areas in the left image of Figure 4.

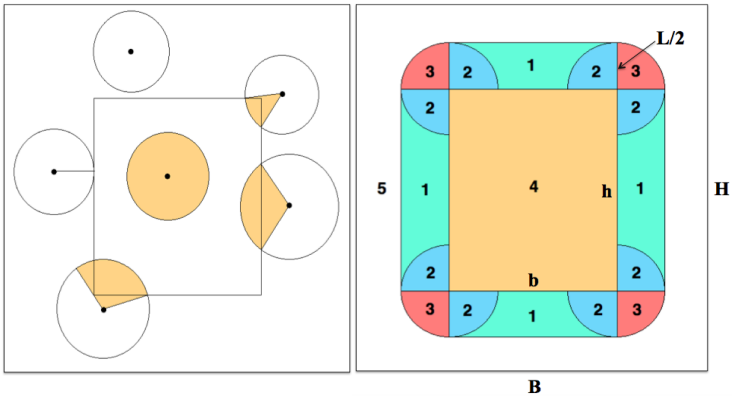

Figure 4. Left: center of the crack is represented by black dot; shaded areas are "detectable angles". Right: Zones 1 to 4 are the areas with different detection properties; a crack centered in Zone 5 will not be detected.

Based on above discussion, five zones with different detection properties are identified for the crack center, and they are shown in the right image of Figure 4. The circles of Zones 2 and 3 have radii of $L/2$. These five zones are used to find the analytical and numerical solutions for POD, but also to interpret and understand the POD relationship with crack length. According to the total probability theory, the POD for a given crack with length L is expressed as follows:

$$POD(L) = \sum POD(L|A_i)P(A_i) \quad (1)$$

where A_i (i=1 to 5) are the above identified Zones 1-5, $P(L|A_i) = \frac{1}{A_i}\iint \frac{\theta_i}{\pi} dxdy$, $P(A_i) = \frac{A_i}{A_{total}}$, and A_{total} is the area of the sensing sheet (BxH).

The above analytical solution can be presented in a closed form for single-sensor scenario only, and it would be too complex to extend to multiple-sensor scenarios. Hence, numerical solutions were built based on Monte Carlo simulations (MCS) to overcome this limitation. Two MCS were created – the first based on "detectable angles" (see Figure 4), and the second based on testing whether the crack intersected the sensor (see Figure 3). An additional point of validation is the fact that for zero crack length (crack collapses into a point), the POD is equal to probability that the crack will occur within the sensor area, which is in turn equal to the area of sensor divided by the area of surface (or the sensing sheet area). This statement is also true for multi-sensor scenarios, i.e. for n sensors ($n \geq 1$):

$$POD(L=0) = \frac{Area\ of\ sensor(s)}{Area\ of\ sensing\ sheet\ surface} = \frac{nbh}{BH} \quad (2)$$

3. Results and parametric studies

The research of this section addresses following question: 'how do the sizes of the non-instrumented areas influence the reliability in damage detection'. The POD for the single sensor scenario is assessed including the analytical and both MCS solutions. Then results from multiple-sensor scenarios (2, 4, 9, and 16 sensors) and variable surface area sizes were presented and compared.

3.1 Single sensor scenario

The analyzed single-sensor scenario is similar to the ones shown in Figures 3 and 4. To simplify the analysis, a square surface area was considered (B=H=20 mm). The relationship between the POD and crack length, determined based on analytical and both MCS solutions is shown in Figure 5. The black polygonal dashed line represents the analytical solution based on Equations 1, while the two other lines (dotted and solid) represent the numerical solutions obtained by MCS. The analytical and numerical solutions show very consistent results, which validates the numerical solutions. For relatively small cracks (0 to ~8 mm for the case presented in Figure 5), the POD increases rapidly as the crack length increases. However, for longer crack lengths (~8 to 14 mm for the presented case) the rate of increase of POD becomes smaller, and reaches a plateau (value of 0.78), after which there is no increase further in POD regardless the size of crack. This indicates that for a given surface area and a given size of the sensor, there is a maximum POD that could be reached. For single-sensor scenario, it is denoted by $POD_{max(1)} = 0.78$ (for area B=H=20 mm and sensor size 11x14 mm).

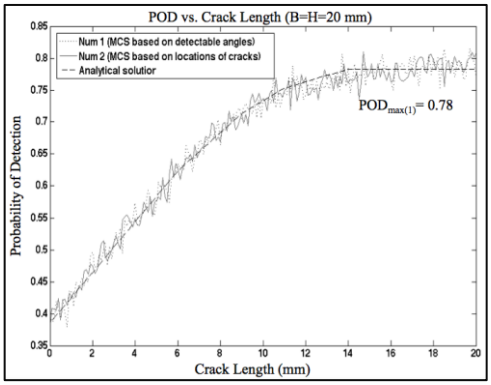

Figure 5. Results of analytical solution (smooth line) and two MC simulations (zigzag lines) for *POD* in a given surface area.

Figure 6 shows diagrams for the POD for varying lengths B and H, in which the crack lengths change from 5 mm to 10 mm. The image to the left shows the analytical solution, and the image to the right shows results of numerical (MCS) solution based on crack intersection criteria. The two diagrams show excellent agreement.

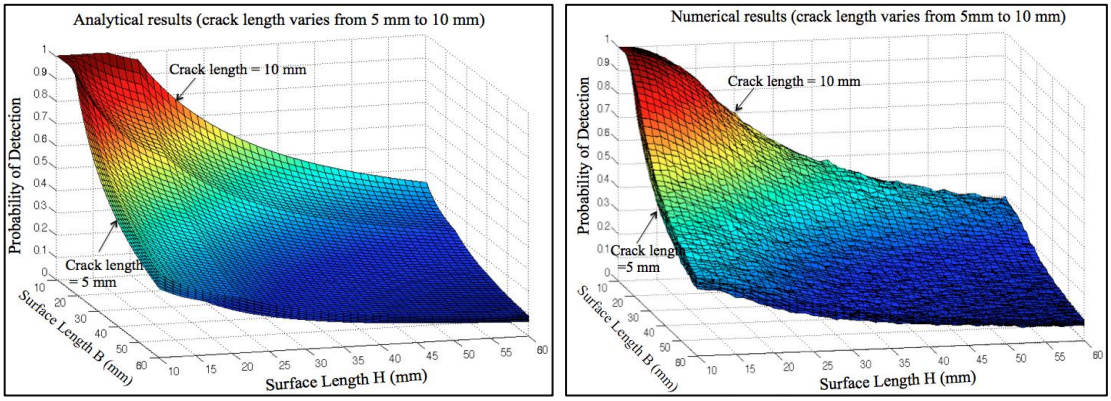

Figure 6. Left: Analytical results of POD against varying B and H of different crack lengths. Right: Numerical results of POD against varying B and H of different crack lengths.

To simplify the 3D presentation of the diagrams from Figure 6, a 2D presentation is created in Figure 7 for the special case where B=H. The left and right images of Figure 7 show respectively

the analytical and numerical solution of POD against varying square area of sensing sheet (B=H) for different crack lengths (L ranges between 5 mm and 10 mm). The POD decreases as the surface area increases, and the POD increases as the crack length increases for a given surface area. The figure indicates in general that for a square surface area of 144 mm^2 or less, the POD is practically equal to 1, since the sensor is bigger than the area. However, when the surface area is more than 625 mm^2, the POD is smaller than 0.5.

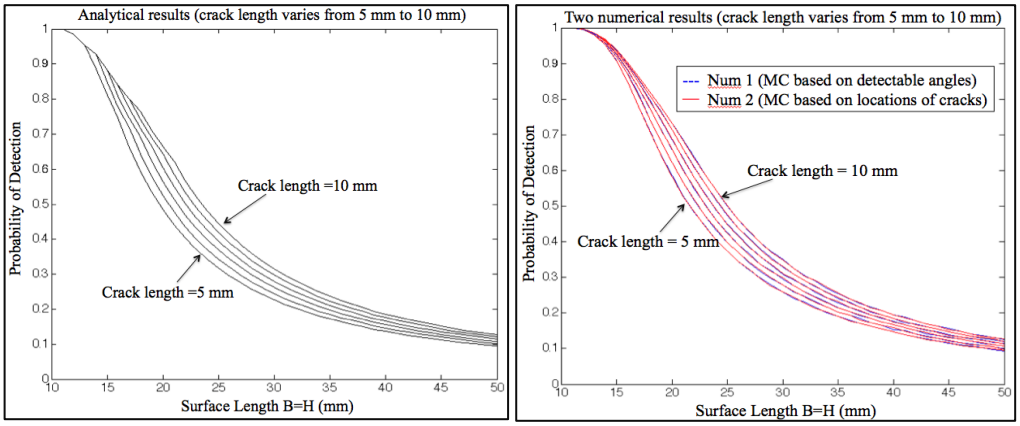

Figure 7. Left: Analytical results of POD against changes in B=H of different crack lengths. Right: Numerical results of POD against changes in B=H of different crack lengths.

3.2 Two-sensor scenario

For multiple-sensor scenarios only MCS based on crack intersection criteria can be used (see Section 2). To examine the relationship between the POD and the size of the crack length, but also to perform additional validation of the MCS, we study first the two-sensor scenario. Thus, two sensors (size 11x14 mm) are placed symmetrically in the arbitrarily chosen surface area 56x34 mm, as shown in Figure 8, and the relationship between the POD and the crack length is determined using MCS, similar to a single scenario case.

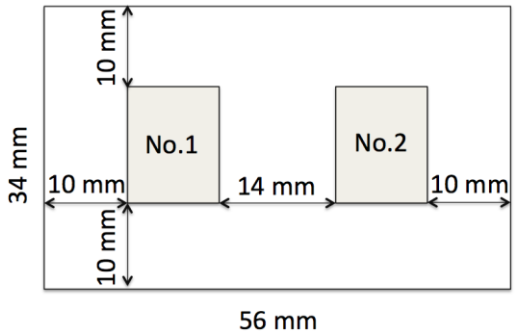

Figure 8. Example of sensing sheet design with two-sensor scenario.

Keeping the sensing sheet area constant and gradually changing the crack length, the relationship POD vs. crack length is assessed for this two-sensor scenario, as shown in Figure 10. The maximum POD is denoted by $POD_{max(2)} = 0.63$ (for BxH=56x34 mm, and bxh=11x14 mm). The validation of MCS was examined by checking the probability value when crack length equals 0 (see Equation 2 in Section 2), and the comparison between the theoretical value and MCS was consistent (see circled area and associated equation in Figure 10).

3.3 Four-, nine-, and sixteen-sensor scenarios

From the two-sensor scenario to the four-sensor scenario, we doubled the number of sensors and the

sensing sheet area. The layout of sensors is shown in left image of Figure 9. The relative locations of the four sensors are kept the same as in two-sensor case, and they are located in a surface area of 56x68 mm. All dimensions are described in Figure 9 (left).

For comparison purposes, the results of PODs vs. crack length are for the two- and four-sensor scenario cases given in Figure 10. The comparison shows the expected good agreement for crack lengths shorter than 20 mm, and this further validates the MCS (the Expression 3 yields the same result for the zero crack length). The maximal POD of the four-case scenario $POD_{max(4)} = 0.64$, is slightly higher than the maximal POD of the two-sensor scenario $P_{(2)} = 0.63$. This implies that simply doubling number of sensors and the surface area does not affect significantly the maximum probability of damage detection, provided that the relative locations of sensors remain unchanged.

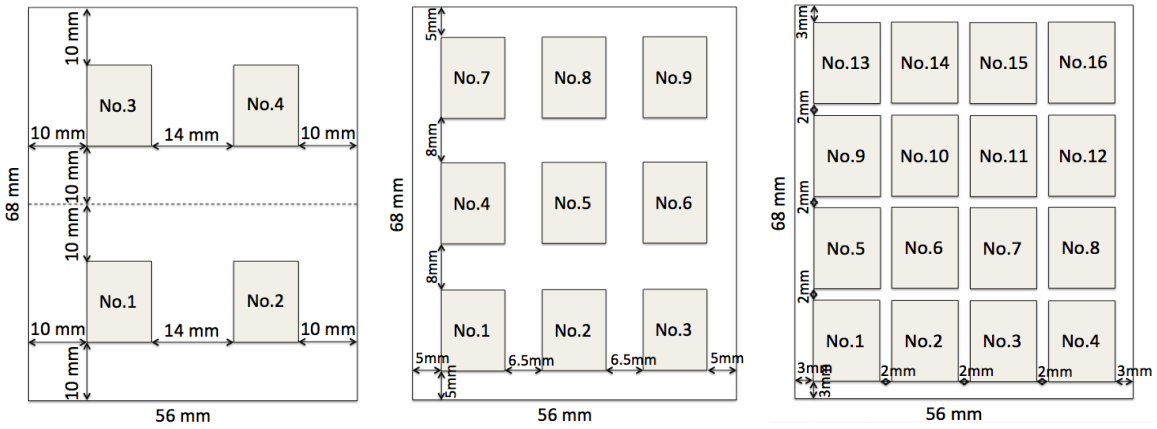

Figure 9. Examples of sensing sheet designs with multiple sensors. Left: Four-sensor scenario; Middle: Nine-sensor scenario; and Right: Sixteen-sensor scenario.

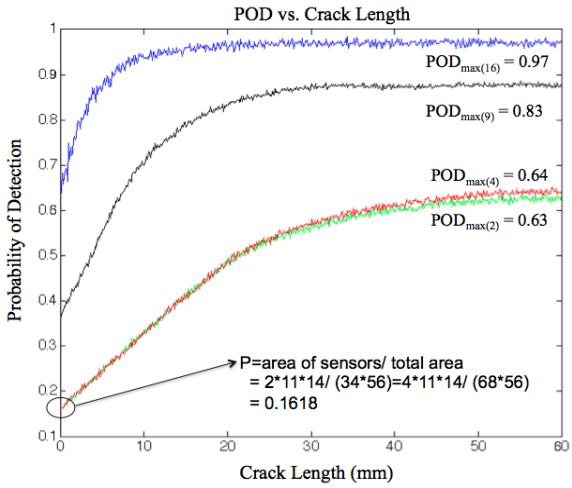

Figure 10. POD vs. crack length for two-, four-, nine-, and sixteen-sensor scenario calculated by MCS.

Considering that all the previous cases validated our MCS approach, we further studied the effect of an increased number of sensors on the POD for a sensing sheet area of constant size. Therefore, the nine-sensor scenario and sixteen-sensor scenario are studied as per Figures 9 Middle and Right, respectively. The surface area and the sizes of individual sensors are kept the same as for four-sensor scenario (*BxH*=56x34 mm, and *bxh*=11x14 mm). The validation of the MCS by Expression 3 was judged as sufficient. The results are presented in Figure 10. It can be seen that all graphs have similar patterns, and the maximum POD increases as the number of sensors increases.

4. Conclusions

This research proposes a probabilistic approach for determination of relative sensor size and number on innovative sensing sheets based on large area electronics. General principles were derived based on the notion of Probability of Detection (POD) and geometrical probability analysis, and validated using Monte Carlo simulations (MCS). Several methods were used in the course of the work to confirm the reliability of the MCS.

Analytical expressions were derived for single sensor within the sensing sheet and five influence zones were identified. POD increases as crack length increases and there is a maximum POD when crack length reaches a critical value. The POD decreases as surface area increases, which indicates that the sensors in the sensing sheet should not be spaced too far apart. The influence of different shapes (varying surface lengths) of the surface area on the POD is also studied. As the number of sensors increases, the maximum POD indeed grows, while doubling number of sensors and surface area simultaneously would not affect significantly the maximum POD, given that the relative locations of sensors remain unchanged.

The significance of this research is twofold. First, it provides the end users with means to evaluate the probability that the damage of certain size is present on structure; and second, it provides very important conclusions regarding the arrangement of sensors in the sensing sheet that can serve as guidelines for establishing the manufacturing design of the sensing sheets. The broader impact of the study reflects in the fact that the derived principles can be generally applied beyond the scope of the sensing sheet and used in many applications where an array of sensors is applied to an area of structure.

5. Acknowledgments

This research was supported by the Princeton Institute for the Science and Technology of Materials (PRISM), and in part by the USDOT-RITA UTC Program, grant No. DTRT12-G-UTC16, enabled through the Center for Advanced Infrastructure and Transportation (CAIT) at Rutgers University. The authors would like to thank S-T. E. Tung, Prof. N. Verma, Y. Hu, L. Huang, N. Lin, W. Rieutort-Louis, J. Sanz-Robinson, T. Liu, Prof. J. C. Sturm, and Prof. S. Wagner for their precious advice and help in the project.

References

[1] Yao, Y. and Glisic, B. (2012). "Reliable damage detection and localization using direct strain sensing," *Bridge Maintenance, Safety, Management, Resilience and Sustainability – Proceedings of the Sixth International IAMBAS Conference on Bridge Maintenance, Safety and Management*, pp. 714-721.

[2] Posenato, D., Lanat, F., Inaudi, D. and Smith, I. F. C. (2008). "Model-free data interpretation for continuous monitoring of complex structures", *Advanced Engineering Informatics*, Vol. 22, No. 1, pp. 135-144.

[3] Glisic, B., Chen, J. and Hubbell, D. (2011). "Streicker Bridge: a comparison between Bragg-gratings long-gauge strain and temperature sensors and Brillouin scattering-based distributed strain and temperature sensors", *SPIE Smart Structures/NDE 2011*, 7981-81, San Diego, CA, USA.

[4] Glisic, B. and Yao, Y. (2012). "Fiber optic method for health assessment of pipelines subjected to earthquake-induced ground movement", *Structural Health Monitoring*, Vol. 11, No. 6, pp. 696-711.

[5] Arias, A. C., MacKenzie, J. D., McCulloch, I., Rivnay, J. and Salleo, A. (2010). "Materials and applications for large area electronics: Solution-based approaches," *Chemical Reviews*, Vol. 110, No. 1, pp. 3–24.

[6] Someya, T., Pal, B., Huang, J., and Katz, H. E. (2008). "Organic semiconductor devices with enhanced field and environmental responses for novel applications," *MRS Bulletin*, Vol. 33, No. 7, pp. 690–696.

[7] Glisic, B. and Verma, N. (2011). "Very dense arrays of sensors for SHM based on large area electronics," *Structural Health Monitoring 2011: Condition-Based Maintenance and Intelligent Structures – Proceedings of the 8th International Workshop on Structural Health Monitoring,* 2, pp. 1409-1416.

[8] Coppe, A., Haftka, R. T., and Kim, N. (2009). "Optimization of Distribution Parameters for Estimating Probability of Crack Detection." *Journal of Aircraft*, Vol. 46, No. 6, pp. 2090-97.